



# Adipose-derived mesenchymal stem cells combined with platinum nanoparticles accelerate fracture healing in a rat tibial fracture model

Chuan-Jie Chen<sup>1</sup>, Yuan Feng<sup>2</sup>, Lin Jin<sup>1</sup>, Xin Wang<sup>1</sup>, Li-xiao-zi Xu<sup>3</sup>, Jia-Mei Lin<sup>4</sup>, Li-Wen Feng<sup>5</sup>, Li-Na Liu<sup>6</sup>, Zhiyong Hou<sup>1</sup>

<sup>1</sup>Department of Orthopaedic Surgery, Third Hospital of Hebei Medical University, Shijiazhuang, China; <sup>2</sup>Department of Hepatobiliary Surgery, The Third Affiliated Hospital of Sun Yat-sen University, Guangzhou, China; <sup>3</sup>Department of Plastic Surgery, Foshan Fosun Chancheng Hospital, Foshan, China; <sup>4</sup>Institute of Pharmaceutics, School of Pharmaceutical Sciences (Shenzhen), Sun Yat-sen University, Shenzhen, China; <sup>5</sup>Boji Medical Biotechnological Co., Ltd., Boji Pharmaceutical Research Center, Guangzhou, China; <sup>6</sup>General Medical Department, Tianjin Nankai Hospital, Tianjin, China

**Contributions:** (I) Conception and design: CJ Chen, Y Feng; (II) Administrative support: Z Hou; (III) Provision of study materials: CJ Chen, LX Xu, JM Lin, LW Feng; (IV) Collection and assembly of data: CJ Chen, L Jin, LN Liu; (V) Data analysis and interpretation: CJ Chen, X Wang; (VI) Manuscript writing: All authors; (VII) Final approval of manuscript: All authors.

**Correspondence to:** Zhiyong Hou. Department of Orthopaedic Surgery, Third Hospital of Hebei Medical University, Shijiazhuang, China. Email: drzyhou@gmail.com.

**Background:** At present, bone union delay or failure remains challenging for clinicians. It has been reported that adipose-derived mesenchymal stem cells (ADMSCs) offer a promising way to promote bone fracture healing. In recent years, nanomaterials have been applied in regenerative medicine. This study aimed to investigate whether ADMSCs combined with platinum nanoparticles (PtNPs) could further improve fracture healing on the basis of ADMSCs.

**Methods:** ADMSCs were co-cultured with PtNPs *in vitro* to investigate the effect of PtNPs on the differentiation of ADMSCs. Twenty Sprague-Dawley (SD) rats were randomly divided into four groups (with five rats in each group). The left tibias of all rats were fractured. Phosphate-buffered saline (PBS), PtNPs, ADMSC, and ADMSC mixed with PtNPs were then injected into the fracture sites based on the group classifications. The fracture was monitored by X-ray immediately after the fracture and on days 14 and 28 post-fracture. The tibias of the rats were subsequently harvested after the last X-ray and evaluated by micro computed tomography (micro-CT), histological analysis, and immunohistochemical detection.

**Results:** PtNPs significantly enhanced the osteogenic differentiation of ADMSCs *in vitro*. On days 14 and 28 post-fracture, the radiographic score of the ADMSC + PtNPs group was higher than that of the ADMSC group, the score of the ADMSC group was higher than that of the PtNPs and control groups, and there was no significant difference between the PtNPs and control groups. Micro-CT confirmed that combined ADMSCs with PtNPs were more effective than using ADMSCs alone in promoting fracture healing. The histological and immunohistochemical results further supported this conclusion.

**Conclusions:** Our findings demonstrated that PtNPs could promote osteogenic differentiation of ADMSC *in vitro*. ADMSCs combined with PtNPs could accelerate fracture healing further *in vivo* and are a promising a potential method for the treatment of fracture healing.

**Keywords:** Platinum nanoparticles (PtNPs); adipose-derived mesenchymal stem cells (ADMSCs); bone healing

Submitted Feb 15, 2022. Accepted for publication Apr 02, 2022.

doi: 10.21037/atm-22-1196

**View this article at:** <https://dx.doi.org/10.21037/atm-22-1196>

## Introduction

Bone fractures are among the most common injuries in the emergency room. It has been estimated that 5–10% of fractures progress to nonunion. The risk factors for fracture nonunions are various and can be divided into patient-dependent factors (e.g., age, gender, body mass index, smoking) and patient-independent factors (e.g., open fracture, open reduction, infection) (1). Nonunion treatment remains a challenge for orthopaedic trauma surgeons, as it can lead to morbidity, prolonged hospitalization, and substantial social resource consumption (2,3). With the aging society, the proportion of the elderly population will increase, and the incidence of fracture nonunion may also increase accordingly.

Autologous bone graft (ABG) has been the gold standard treatment for nonunion over the past century due to its histocompatibility, osteo-inductive, and osteoconductive properties (4). However, ABG also has significant drawbacks such as limited quantity, additional surgery for bone harvesting, and complications of the donor site (5,6). Therefore, it is critical to develop novel therapies to improve the fracture healing and treat nonunion.

Mesenchymal stem cells (MSCs) have been applied in tissue regeneration for decades as a result of their differentiation potential (7-9). MSCs are known to differentiate into osteoblasts to enable bone formation, and are used to treat fracture nonunion and bone defects (10,11). Bone marrow MSCs (BMMSCs) were first used to treat a large bone defect in 1998 and had previously been the main object of research (12). However, the accessibility, quantity, and donor site morbidity of BMMSCs have been problematic for researchers. Adipose-derived MSCs (ADMSCs), which can solve these problems, have attracted increasing attention and have been used in the field of bone regeneration (13-15). There are numerous studies aimed at developing biomaterials that promote fracture healing, and it has been found several kinds of nanomaterials could modulate the osteogenic differentiation of MSCs (16-23). Through literature search, there are no *in vivo* studies on combining adipose stem cells with platinum nanoparticles (PtNPs) for fracture healing.

In the present study, rats with tibial fractures were treated with ADMSCs combined with PtNPs, and were then evaluated with radiography, micro computed tomography (micro-CT), histology, and immunohistochemistry to investigate the effect of the combination of ADMSCs and PtNPs on fracture healing. Our data indicated that PtNPs

could promote the osteogenic differentiation of ADMSCs *in vitro* and the combination of ADMSCs and PtNPs could accelerate fracture healing in a rat tibial fracture model. We present the following article in accordance with the ARRIVE reporting checklist (available at <https://atm.amegroups.com/article/view/10.21037/atm-22-1196/rc>).

## Methods

### *Synthesis and characterization of platinum nanoparticles (PtNPs)*

The PtNPs were obtained as described in the literature (24). Briefly, 1 mL hexachloroplatinic acid (16 mmol) aqueous solution and 1 mL trisodium citrate (40 mmol) aqueous solution were added into 32 mL ultrapure water and stirred for 30 min at room temperature. Next, 200  $\mu$ L sodium borohydride (0.01 mmol) aqueous solution was added dropwise after placing the mixture in an ice bath for 15 min. The reaction proceeded for 4 h at room temperature. Following the addition of 250 mL of acetone, the resulting solution was sonicated and centrifuged at 30,000 rpm for 30 min. The PtNPs then were dried under vacuum and collected. A high resolution-transmission electron microscope (JEOL, Tokyo, Japan) was used to analyze the PtNPs.

### *Isolation and culture of ADMSCs*

ADMSCs were isolated from adipose tissue according to the methods described previously (25). Briefly, human adipose aspirated wastes were obtained from healthy volunteers at The Third Affiliated Hospital of Sun Yat-sen University. The study was conducted in accordance with the Declaration of Helsinki (as revised in 2013). The cell experiment was approved by ethics board of The Third Affiliated Hospital of Sun Yat-sen University [No. (2020) 02-585] and informed consent was taken from all the volunteers. The adipose tissue was minced, rinsed twice with phosphate-buffered saline (PBS), and digested with collagenase type I. Dulbecco's Modified Eagle's Medium-Low Glucose (DMEM-LG) containing 10% fetal bovine serum (FBS) was used to neutralize the collagenase. Next, the cells were washed with DMEM-LG and seeded in tissue culture flasks containing DMEM/10%FBS. When the monolayer of adherent cells reached 70–80% confluence, cell passaging was performed. Subsequently, differentiation assays were used to verify the stem cell characteristics of the

ADMSCs.

### *Cell proliferation assay in vitro*

ADMSCs ( $1 \times 10^3$  cells) were incubated in a 96-well plate without or with PtNPs (5, 10 mg) before the Cell Counting Kit-8 (CCK-8) assay (26). The cells were cultured for 0, 1, 2, 3, 4, 5, 6, and 7 days. CCK-8 reagent (Beyotime, Shanghai, China) was added following manufacturer's instructions for cell activity measurement. The absorbance value at 450 nm on a microplate reader (BioTek, USA) was recorded.

ADMSCs were seeded in 24-well plates in a medium with 10% FBS for 24 h. Then, the cells were cultured using serum-free medium, and PtNPs (5 and 10 mg) were added to the test groups for 48 h. Next, the 5-ethynyl-2'-deoxyuridine (EdU)-labelling reagent (Beyotime, Shanghai, China) was added following manufacturer's instructions. After 6 hours, the cells were fixed with paraformaldehyde for 30 min and then immersed in 2 mg/mL glycine solution for 5 min. The cells were subsequently incubated with 0.5% TritonX-100 in PBS at room temperature for 20 min. The cells were detected using an EdU Kit (Beyotime, Shanghai, China) according to the instruction manual.

### *Cell differentiation in vitro*

ADMSCs were cultured with differentiation medium without or with PtNPs (5, 10 mg) for 21 days. Osteogenic, adipogenic, and chondrogenic differentiation media were purchased from Cyagen Biosciences (USA). The medium was changed every 3 days until day 21. After that ADMSCs were fixed and stained with Alizarin Red S solution, Oil Red O solution, or Alcian Blue solution, washed with distilled water and examined under light microscope.

### *Animals*

Twenty mature male Sprague-Dawley (SD) rats (6 weeks old, 180–200 g) were obtained from Sipeifu Biotechnology Co., Ltd. (Beijing, China). Animal experiments were performed under a project license (No. Z2022-011-1) granted by Ethics Committee of Third Hospital of Hebei Medical University, in compliance with guidelines of Third Hospital of Hebei Medical University for the care and use of animals. SD rats were randomly divided into control, PtNPs, ADMSC, and ADMSC + PtNPs groups ( $n=5$  in each). Animals were housed in a light and temperature controlled environment with free access to food and water.

### *Rat fracture model*

The SD rats were anesthetized by isoflurane inhalation. The left lower limbs of the rats were depilated with razor and disinfected. A 10 mm long longitudinal incision was made from the medial portion of the tibial plateau to the medial malleolus. Following separation of the fascia, muscle, and periosteum, a transverse osteotomy was performed using a saw 5 mm below the tibial tubercle, and then fixed with a 1 mm Kirschner wire in retrograde. Next, 50  $\mu$ L PBS, 30 mg/kg PtNPs (dissolved in 50  $\mu$ L PBS),  $1 \times 10^6$  ADMSC (dissolved in 50  $\mu$ L PBS), and 30 mg/kg PtNPs mixed with  $1 \times 10^6$  ADMSC (dissolved in 50  $\mu$ L PBS) were injected into the fracture sites based on the group classifications using a 1-mL syringe. The fascia and skin were then sutured with a 5-0 suture, the incision was wrapped with sterile gauze, and the outcome was evaluated at subsequent time points. Intermuscular penicillin (100,000 IU/mL, 1 mL/kg) was administered before and at 2 days post-fracture in all rats.

### *Radiographic and micro-CT analysis of fracture sites*

Radiography was performed for each rat immediately after the surgery and on days 14 and 28 postoperatively. X-ray images were evaluated by imaging specialists. The radiographic images were scored as follows: (I) no apparent hard callus; (II) slight intramembranous ossification; (III) hard callus without bridging of the fracture gap and fracture line is apparent; (IV) hard callus with bridging of the fracture gap and fracture gap is noticeable; (V) unclear boundary between the newly formed hard callus and existing cortical bone; and (VI) remodeling (27).

The rats' tibias were harvested right after the last X-ray, following removal of the K-wires, and fixed in 4% paraformaldehyde solution for 24 h. Two rats were randomly selected from each group for micro-CT analysis. The rats' tibias were scanned using a micro-CT system [Siemens Inveon Positron Emission Tomography/computed tomography (PET/CT), Germany]. The scan protocol was set as below: 18-mm isometric voxel size, 500  $\mu$ A, and 80 kV. The fracture line was taken as the midpoint reference, a total of 200 slices were analyzed. The callus was drawn manually as a region of interest (ROI), and then the volume fractions bone volume/total volume (BV/TV) and bone mineral density (BMD) were analyzed by Multimodal 3D Visualization. The three-dimensional images were generated by Multimodal 3D Visualization version 3.3 (Bruker-microCT, Germany).

### *Histology and immunohistochemistry*

The tibia specimens fixed with formaldehyde were decalcified in 10% ethylenediaminetetraacetic (EDTA) at room temperature for 2 months (with solution change every 3 days) and then embedded in paraffin. The tibias were then sliced along the longitudinal axis (3- $\mu$ m slices), and routine haematoxylin and eosin (H&E) and safranin O staining were performed to analyze the histologic differences (28).

For immunohistochemical analysis, sections of paraffin-embedded tibia specimens were dewaxed by conventional method. The expression of Runt-related transcription factor 2 (Runx2) and osteocalcin (OCN) was detected to assess the osteogenesis of the tibia. The positive stained tissues were observed under a light microscope (29).

### *Statistical analysis*

Data analysis was performed using SPSS (IBM, USA) for Windows version 21.0. All experiments were conducted in triplicate and the data were expressed as means  $\pm$  standard deviation and analyzed using the Student's *t*-test.  $P < 0.05$  was considered statistically significant.

## **Results**

### *PtNPs promote osteogenic differentiation of ADMSCs in vitro*

First, PtNPs nanoparticles were synthesized according to the literature. The mean diameter of PtNPs averaged 5 nm with spherical sharp, which was confirmed by TEM (Figure 1A). At the same time, we obtained primary ADMSCs from human adipose tissue. The stem cell characteristics of ADMSCs were confirmed by differentiation assays (Figure 1B). PtNPs had no effect on the proliferation of ADMSCs, as verified by CCK-8 and EdU test (Figure 1C,1D). Compared to ADMSCs without PtNPs, the calcium mineralization of ADMSCs co-cultured with PtNPs (5, 10 mg) was significantly enhanced on day 21, which was confirmed by Alizarin red staining. Also, the calcium mineralization degree was dose-dependent. In contrast, PtNPs had no significant effect on the differentiation of ADMSCs into chondrocytes and adipocytes, as shown by Alcian Blue staining and Oil Red O staining (Figure 1E).

### *PtNPs can enhance the effect of ADMSCs on fracture healing in vivo*

We found PtNPs that could promote the osteogenic

differentiation of ADMSCs *in vitro*. We speculated that PtNPs can enhance the role of ADMSCs in promoting fracture healing *in vivo*, so we applied ADMSCs combined with PtNPs *in vivo*. We first established a rat tibia fracture model and divided the rats into control (PBS), PtNPs, ADMSC, and ADMSC combined with PtNPs groups, and the fracture healing process was monitored by radiology. The postoperative X-ray showed that the fractures of all rats were transverse fractures, and were fixed with Kirschner wires. The condition of all the rats was good before and after the operation, and no difference was observed between the groups (Figure 2A). There was also no difference in the radiographic score of each group immediately post-fracture ( $P > 0.05$ ) (Figure 2B).

X-ray examination was performed at 14 days post-fracture; compared to the other three groups, the fracture line of the ADMSC + PtNPs group was blurred. The callus of the ADMSC group was relatively larger than that of the PtNPs and control groups (Figure 2A). Furthermore, the radiographic score of the ADMSC + PtNPs group was higher than that of the ADMSC group ( $P < 0.05$ ), and the radiographic scores of these two groups were higher than those of the control and PtNPs groups ( $P < 0.05$ ). Also, there was no significant difference between the PtNPs and control groups ( $P > 0.05$ ) (Figure 2B).

X-rays were taken 28 days after fracture; the fracture remodeling in the ADMSC + PtNPs group was basically completed and the fracture line had disappeared. The fracture line in the ADMSC group was relatively blurred compared with the PtNPs and control groups. The fracture line in the PtNPs and control groups was still visible (Figure 2A). In terms of radiographic score, those of the ADMSC + PtNPs group were higher than the ADMSC group ( $P < 0.05$ ), and these two groups were also significantly higher than the PtNPs and control groups ( $P < 0.05$ ). Also, there was no significant difference between the PtNPs and control groups ( $P > 0.05$ ) (Figure 2B).

The rats were sacrificed on day 28 post-fracture, and tibia specimens were taken for micro-CT. BMD (an indicator of bone strength) and BV/TV (an indicator of changes in new bone mass) were calculated. The tomographic observation of the three-dimensional (3D) reconstructed images of fracture sites and the newborn callus were consistent with the X-ray findings (Figure 3A,3B). Among the four groups, the BV/TV value of the ADMSC + PtNPs group was the highest. The BV/TV value of the ADMSC group was higher than that of the PtNPs and control groups. Moreover, there was no significant difference between the

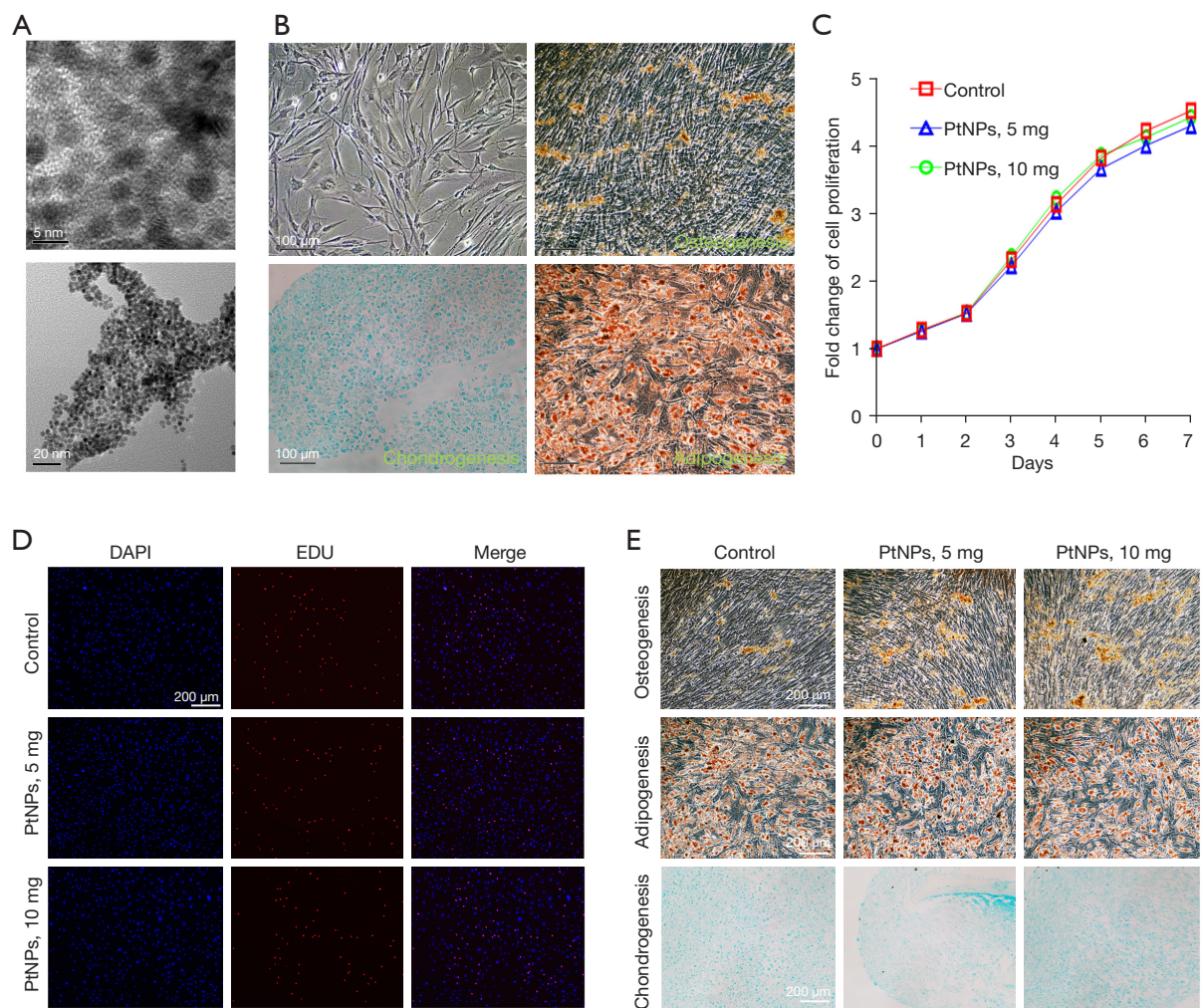


**Figure 1** Characterization of PtNPs. Proliferation and differentiation of ADMSCs co-cultured with PtNPs. (A) TEM images of PtNPs; (B) characteristics of the ADMSCs and the differentiation potential of osteogenic (Alizarin red staining), chondrogenic (Alcian Blue staining) and adipogenic (Oil Red O staining) of the ADMSCs. (C) Detection of ADMSC viability with CCK-8 assay in the presence of PtNPs (5, 10 mg). (D) Representative images of EdU staining in the presence of PtNPs (5, 10 mg). (E) Effect of PtNPs (5, 10 mg) on the osteogenesis differentiation (Alizarin red staining), adipogenesis differentiation (Oil Red O staining) and chondrogenesis differentiation (Alcian Blue staining) of ADMSCs. PtNP, platinum nanoparticle; ADMSC, adipose-derived mesenchymal stem cell; TEM, transmission electron microscope; CCK-8, Cell Counting Kit-8; DAPI, 4',6-diamidino-2-phenylindole; EDU, 5-ethynyl-2'-deoxyuridine.

PtNPs and control groups ( $P > 0.05$ ). The result further verified that the callus formation is consistent with the X-ray results (Figure 3C). However, we found there was no obvious difference in the BMD values of these four groups ( $P > 0.05$ ) (Figure 3D).

In order to further confirm the above findings, we performed histological analysis of the fracture samples. We found the fracture site of the control and PtNPs groups was partially filled with cartilage matrix and new bone callus,

but part of it was also occupied by granulation tissue. In the ADMSC group, the new callus of the fracture was almost closed, while the fracture in the ADMSC + PtNPs group was almost healed. Considerably more chondrocytes were detected in the control and PtNPs groups compared to the ADMSC + PtNPs and ADMSC groups, which means that the new chondrocytes were not mineralized completely in the control and PtNPs groups. Also, no significant difference was observed between the PtNPs and control

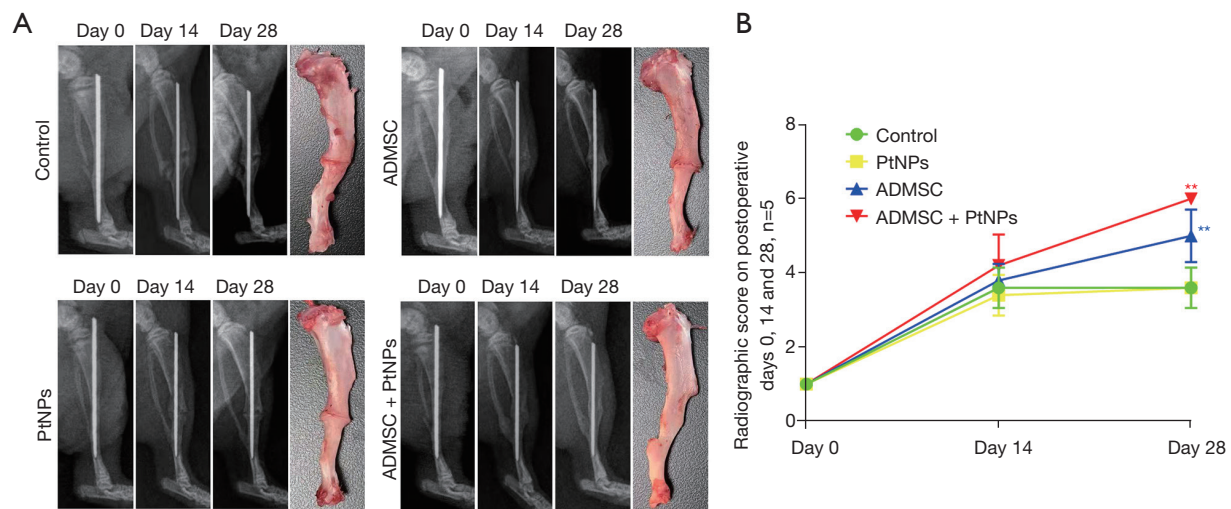


**Figure 2** Radiographic analysis and gross observation of tibial specimens. (A) Series of representative lateral radiographic pictures of the four groups at three different time points (days 0, 14, and 28 post-fracture) and gross observation of tibial specimens. (B) Radiographic score on days 0, 14, and 28 post-fracture (n=5). \*\*, treatment group (ADMSC and ADMSC + PtNPs group). PtNP, platinum nanoparticle; ADMSC, adipose-derived mesenchymal stem cell.

groups. In the ADMSC group, most of the callus had been calcified and the continuity of the cortical bone was basically restored. In the ADMSC + PtNPs group, significantly less chondrocytes could be detected and the callus was almost calcified (Figure 4A).

Runt-related transcription factor 2 (Runx2, a biochemical marker of osteoblast differentiation and bone formation) and osteocalcin (OCN, an advanced osteogenic marker produced only by osteoblasts, which can reflect the number of osteoblasts) were detected by immunohistochemistry. The expression of these two indicators was found to be highest in the ADMSC + PtNPs group, which was higher than that of the ADMSC group, and the expression of these two groups were higher than both the PtNPs and control groups. Also, there was no difference between the PtNPs and control groups (Figure 4B).

## Discussion

Fracture healing is a complex regeneration process. In the past, a large number of studies applied MSCs to treat fracture healing, and nanomaterials have been widely used in the field of tissue regeneration (including bone regeneration) (30,31). In this study, we applied ADMSCs combined with PtNPs in a rat tibial fracture model. Compared with ADMSCs alone, the combination of

ADMSCs and PtNPs could further accelerate the fracture healing process.

Bone regeneration is one of the main fields of concern in regenerative medicine. In recent years, MSCs have been used to promote bone healing due to their potential to differentiate into osteocytes (10,11). MSCs can be obtained from bone marrow, adipose tissue, umbilical cord, and many other tissues. The most commonly used source of MSCs for bone regeneration are BMMSCs and ADMSCs due to their higher osteogenic potential; however, which type of MSC is more effective remains unclear (12-15). The isolation of BMMSCs usually yields small numbers of stem cells and the harvest process is invasive. Also, bone marrow cellularity declines with age, which further limits the clinical applications of BMMSCs (32). It has been shown ADMSCs have similar multilineage potential to BMMSCs (33). As a source of MSCs, adipose tissue has several advantages over bone marrow, including larger supply of autogenous tissue and relatively higher osteoblast production (34,35). Fat tissue is probably the richest source of adult stem cells in the human body (36). Compared to other stem cells, ADMSCs can be easily harvested with minimal invasive procedures. Long-term culture will not cause significant chromosomal aberrations of adipose-derived stem cells, and their morphology, immunophenotype, normal division cycle and apoptosis regulation function can be preserved (37).

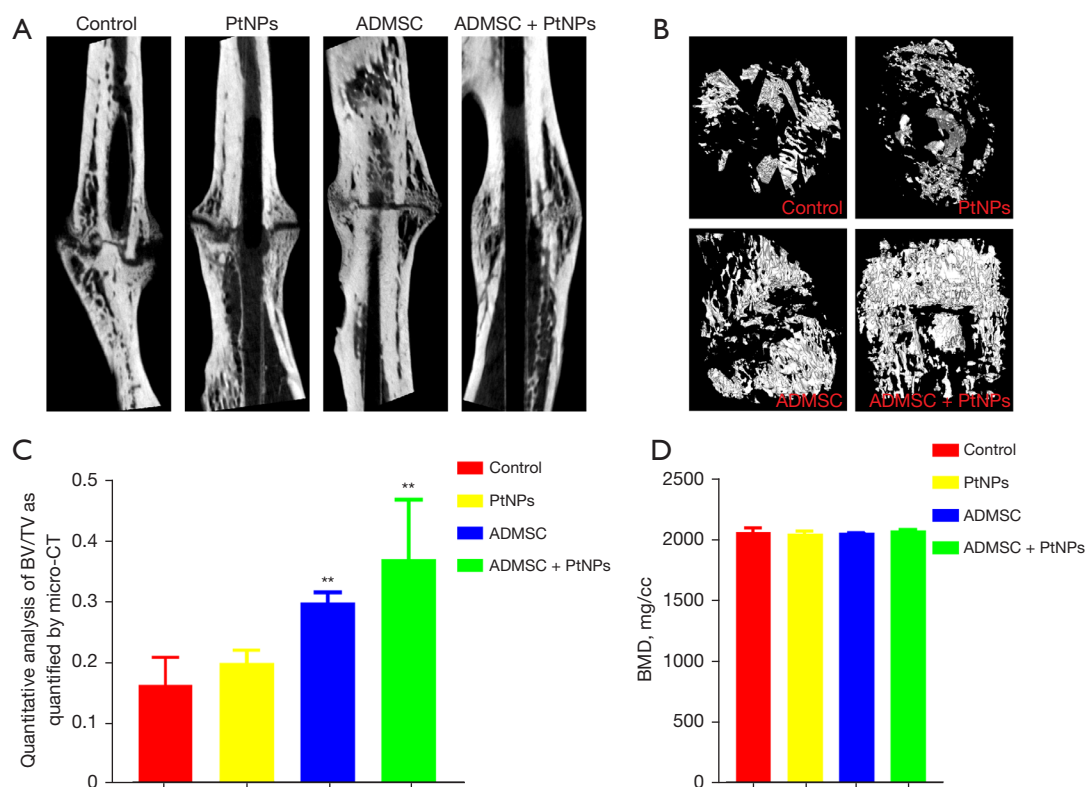


**Figure 3** Micro-CT results. (A) Representative micro-CT 3D reconstructed images on day 28 post-fracture; (B) representative micro-CT 3D reconstructed images of newly formed callus on day 28 post-fracture (original bone removed); (C) quantitative analysis of BV/TV as quantified by micro-CT; (D) quantitative analysis of BMD as quantified by micro-CT. \*\*, treatment group (ADMSC and ADMSC + PtNPs group). PtNP, platinum nanoparticle; ADMSC, adipose-derived mesenchymal stem cell; BMD, bone mineral density; BV/TV, bone volume/total volume.

Long-term cryopreservation of adipose-derived stem cells does not affect their viability, differentiation potential, and immunophenotyped (38). Adipose-derived stem cells have fewer MHC class II molecules and have a lower risk of immunogenicity (39,40). Moreover, it has been demonstrated that BMMSCs fail to repair bone defects, whereas ADMSCs have been shown to successfully enhance bone repair (41-43). Lee *et al.* (44) reported that ADMSCs outperformed BMMSCs in maintaining proliferative capacity. Therefore, ADMSCs should be a better substitute for BMMSCs as a source of bone repair cells. ADMSCs have been used in numerous clinical trials and were licensed in Europe in 2018 for the treatment of patients with Crohn's disease (<http://www.ema.europa.eu>). The success of fracture healing is based on the coordination between bone forming cells and inflammatory cells (45). ACS regulates immunity through direct and indirect communication between cells (46). Macrophages play an important role in the

recruitment and differentiation regulation of MSCs during bone regeneration. Coculture of ASC and macrophages can induce their differentiation into M2 phenotype which play an important role in tissue regeneration, down regulate the expression of pro-inflammatory cytokines and increase the secretion of anti-inflammatory cytokines (45,46). On the other hand, ASCs can also play a role by paracrine soluble mediators, cytokines and growth factors (46).

MSCs may get trapped in the lungs after systemic infusion, leading to thromboembolic events, and thus, local injection of MSC has been advocated (47). In this study, the fracture healing in the ADMSC group was significantly better than that of the control group on X-ray. BV/TV showed that the ADMSC group had more callus. The pathological results showed that there were relatively more chondrocytes at the fracture site in the control group, whereas the fracture in the ADMSC group was almost closed. In addition, the two osteogenic

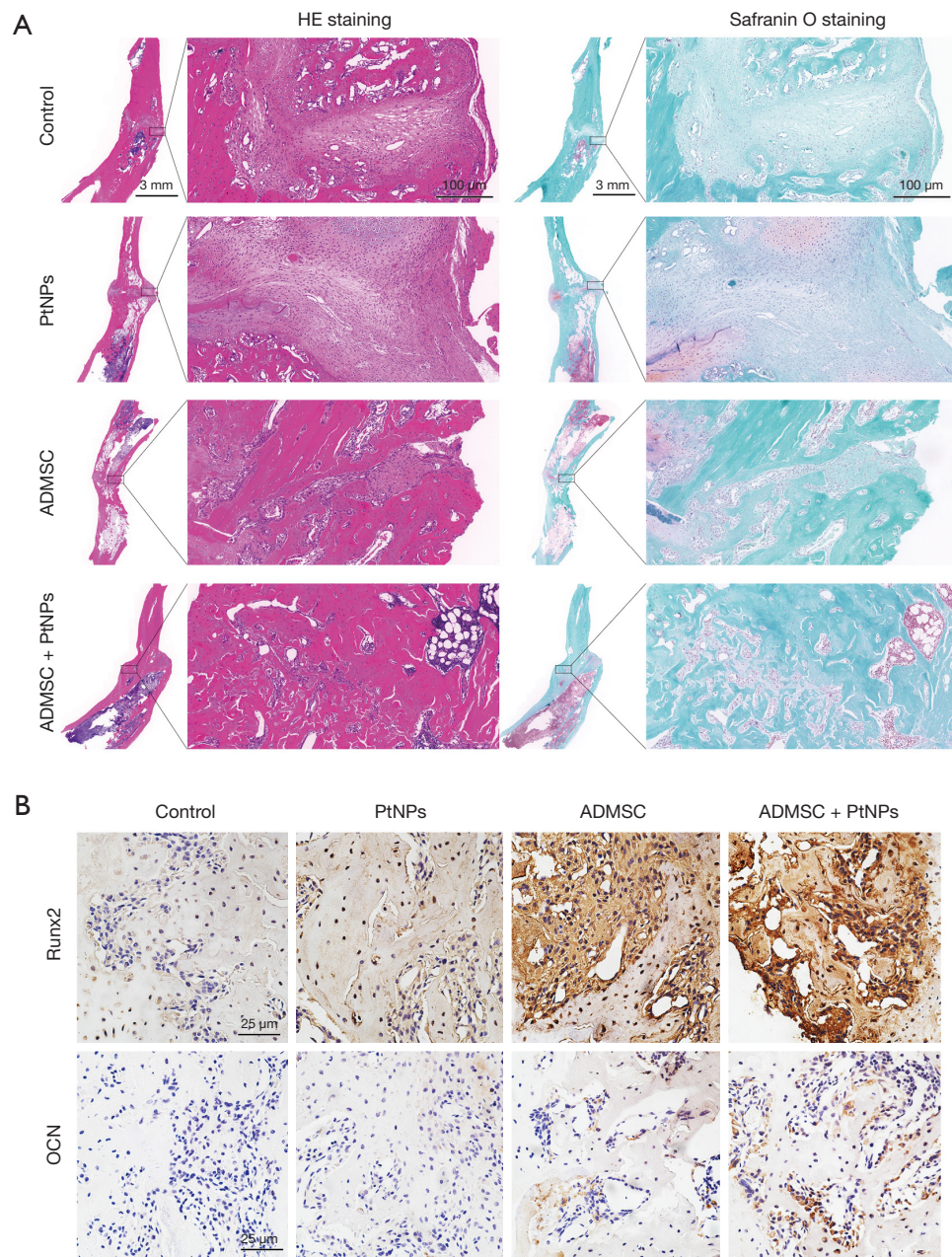


**Figure 4** Histological and immunohistochemical analysis of fracture sites. (A) Histology of the fracture callus stained with HE and Safranin O staining 28 days after fracture. The result of HE staining (left) showed that bone remodeling was completed in the ADMSC + PtNPs group and the bone continuity had been restored. Also, bone remodeling occurred in the ADMSC group, but cracks still could be seen in control and PtNPs groups. Representative sections stained with Safranin O (right) showed that endochondral ossification had almost been achieved in the ADMSC + PtNPs group and partially accomplished in the ADMSC group. In contrast, many uncalcified chondrocytes could be seen in control and PtNPs groups. (B) Immunohistochemical analysis of Runx2 and OCN. The brown colour represents positive staining of Runx2 and OCN. There was nearly no positive staining of Runx2 and OCN in the PtNPs and control groups. Positive staining of Runx2 and OCN could be seen in the ADMSC group. Also, there was more positive staining of Runx2 and OCN in the ADMSC + PtNPs group compared with the ADMSC group. HE, haematoxylin and eosin; ADMSC, adipose-derived mesenchymal stem cell; PtNP, platinum nanoparticle; Runx2, Runt-related transcription factor 2; OCN, osteocalcin.



differentiation indicators, Runx2 and OCN, were detected by immunohistochemistry, and it was found that the osteogenic differentiation of the ADMSC group was better than that of the control group. Therefore, the results showed that ADMSC could prompt the progression of fracture healing.

Nanomaterials have been widely used in tissue regeneration, including bone regeneration. The structure of nanomaterials can regulate cell adhesion, differentiation, proliferation, and promote bone healing (48). It had been found that a variety of nanomaterials (gold nanoparticles, silver nanoparticles, iron oxide nanoparticles) can regulate the expression of related genes by activating different signaling pathways of MAPK and TGF- $\beta$ /BMP, and induce osteogenic differentiation of MSC *in vitro* (17-20,24). Platinum is a harmless metal that is widely used in various industrial products due to its catalytic activity (49). PtNPs are considered non-toxic; however, the toxicity of PtNPs is related to the size, dose, and physico-chemical properties (50). PtNPs, which can inhibit receptor activator of nuclear factor kappa B ligand (RANKL)-induced osteoclast differentiation, have been used to treat ovariectomy-induced osteoporosis (51). In this study, ADMSCs were co-cultured with PtNPs *in vitro*, and we found that the osteogenic differentiation process of ADMSCs was enhanced and positively correlated with the dose of PtNPs. However, when the PtNPs were applied to the fracture site, no significant improvement in fracture healing was observed in comparison to the control, as shown by X-ray, CT, pathology, and immunohistochemistry. Zhang *et al.* (18) reported that mouse MSCs (mMSCs) combined with silver nanoparticles (AgNPs) could promote fracture healing in a mouse fracture model. In this study, we applied ADMSCs combined with PtNPs to a rat tibia fracture model. Twenty-eight days after the fracture, the results of X-ray, CT, and pathology showed that the fractures in the ADMSC + PtNPs group had basically completed reconstruction, whereas in the ADMSC group, the fractures were almost healed, but the reconstruction had not been completed. Furthermore, by detecting the two osteogenic differentiation markers, Runx2 and OCN, it was found that the osteogenesis of the ADMSC + PtNPs group was better than that of the ADMSC group. Therefore, we speculated that PtNPs could further enhance the role of ADMSC in promoting fracture healing *in vivo*. The specific mechanism is still unclear. According to the previous research results of metal nanoparticles on the osteogenic differentiation of stem cells, we speculate that PtNPs may act by affecting some osteogenic signaling pathways, which needs to be

further studied (17-19).

According to our research, transplantation of ADMSCs combined with PtNPs is expected to become a feasible and effective method for treating fracture healing in times to come. With further in-depth research, in the future fracture treatment process, for some patients with relatively high risk of nonunion, whether certain treatment methods to promote fracture healing can be applied preventively to reduce the rate of fracture nonunion. However, there are still some problems that need to be resolved prior to the clinical application of PtNPs combined with ADMSCs, such as whether the effect is related to the number of ADMSCs, optimal dose of PtNPs during application, and the transplantation method. The specific mechanism also needs to be further investigated. We plan to answer some of these questions in the future.

## Acknowledgments

*Funding:* None.

## Footnote

*Reporting Checklist:* The authors have completed the ARRIVE reporting checklist. Available at <https://atm.amegroups.com/article/view/10.21037/atm-22-1196/rc>

*Data Sharing Statement:* Available at <https://atm.amegroups.com/article/view/10.21037/atm-22-1196/dss>

*Conflicts of Interest:* All authors have completed the ICMJE uniform disclosure form (available at <https://atm.amegroups.com/article/view/10.21037/atm-22-1196/coif>). LWF is from Boji Medical Biotechnological Co. Ltd. The other authors have no conflicts of interest to declare.

*Ethical Statement:* The authors are accountable for all aspects of the work in ensuring that questions related to the accuracy or integrity of any part of the work are appropriately investigated and resolved. The study was conducted in accordance with the Declaration of Helsinki (as revised in 2013). The cell experiment was approved by ethics board of The Third Affiliated Hospital of Sun Yat-sen University [No. (2020) 02-585] and informed consent was taken from all the volunteers. This animal study was reviewed and approved under a project license (No. Z2022-011-1) granted by Ethics Committee of Third Hospital of Hebei Medical University, in compliance with guidelines

of Third Hospital of Hebei Medical University for the care and use of animals.

*Open Access Statement:* This is an Open Access article distributed in accordance with the Creative Commons Attribution-NonCommercial-NoDerivs 4.0 International License (CC BY-NC-ND 4.0), which permits the non-commercial replication and distribution of the article with the strict proviso that no changes or edits are made and the original work is properly cited (including links to both the formal publication through the relevant DOI and the license). See: <https://creativecommons.org/licenses/by-nc-nd/4.0/>.

## References

- Andrzejowski P, Giannoudis PV. The 'diamond concept' for long bone non-union management. *J Orthop Traumatol* 2019;20:21.
- Tzioupis C, Giannoudis PV. Prevalence of long-bone non-unions. *Injury* 2007;38 Suppl 2:S3-9.
- Calori GM, Mazza E, Colombo M, et al. Treatment of long bone non-unions with polytherapy: indications and clinical results. *Injury* 2011;42:587-90.
- Gómez-Barrena E, Padilla-Eguiluz NG, Rosset P. Frontiers in non-union research. *EFORT Open Rev* 2020;5:574-83.
- Goulet JA, Senunas LE, DeSilva GL, et al. Autogenous iliac crest bone graft. Complications and functional assessment. *Clin Orthop Relat Res* 1997;(339):76-81.
- Schmidt AH. Autologous bone graft: Is it still the gold standard? *Injury* 2021;52 Suppl 2:S18-22.
- Vasanthan J, Gurusamy N, Rajasingh S, et al. Role of Human Mesenchymal Stem Cells in Regenerative Therapy. *Cells* 2020;10:54.
- Yang L, Li Y, Gong R, et al. The Long Non-coding RNA-ORLNC1 Regulates Bone Mass by Directing Mesenchymal Stem Cell Fate. *Mol Ther* 2019;27:394-410.
- Yang F, Yang L, Li Y, et al. Melatonin protects bone marrow mesenchymal stem cells against iron overload-induced aberrant differentiation and senescence. *J Pineal Res* 2017.
- Grayson WL, Bunnell BA, Martin E, et al. Stromal cells and stem cells in clinical bone regeneration. *Nat Rev Endocrinol* 2015;11:140-50.
- Crane JL, Cao X. Bone marrow mesenchymal stem cells and TGF- $\beta$  signaling in bone remodeling. *J Clin Invest* 2014;124:466-72.
- Bruder SP, Kurth AA, Shea M, et al. Bone regeneration by implantation of purified, culture-expanded human mesenchymal stem cells. *J Orthop Res* 1998;16:155-62.
- Liu J, Zhou P, Long Y, et al. Repair of bone defects in rat radii with a composite of allogeneic adipose-derived stem cells and heterogeneous deproteinized bone. *Stem Cell Res Ther* 2018;9:79.
- Barba M, Di Taranto G, Lattanzi W. Adipose-derived stem cell therapies for bone regeneration. *Expert Opin Biol Ther* 2017;17:677-89.
- Qiu J, Li J, Wang S, et al. TiO<sub>2</sub> Nanorod Array Constructed Nanotopography for Regulation of Mesenchymal Stem Cells Fate and the Realization of Location-Committed Stem Cell Differentiation. *Small* 2016;12:1770-8.
- Lu Z, Roohani-Esfahani SI, Li J, et al. Synergistic effect of nanomaterials and BMP-2 signalling in inducing osteogenic differentiation of adipose tissue-derived mesenchymal stem cells. *Nanomedicine* 2015;11:219-28.
- Wang Q, Chen B, Cao M, et al. Response of MAPK pathway to iron oxide nanoparticles in vitro treatment promotes osteogenic differentiation of hBMSCs. *Biomaterials* 2016;86:11-20.
- Zhang R, Lee P, Lui VC, et al. Silver nanoparticles promote osteogenesis of mesenchymal stem cells and improve bone fracture healing in osteogenesis mechanism mouse model. *Nanomedicine* 2015;11:1949-59.
- Yi C, Liu D, Fong CC, et al. Gold nanoparticles promote osteogenic differentiation of mesenchymal stem cells through p38 MAPK pathway. *ACS Nano* 2010;4:6439-48.
- Bharadwaz A, Jayasuriya AC. Recent trends in the application of widely used natural and synthetic polymer nanocomposites in bone tissue regeneration. *Mater Sci Eng C Mater Biol Appl* 2020;110:110698.
- Li Y, Feng C, Gao M, et al. MicroRNA-92b-5p modulates melatonin-mediated osteogenic differentiation of bone marrow mesenchymal stem cells by targeting ICAM-1. *J Cell Mol Med* 2019;23:6140-53.
- Li Y, Yang F, Gao M, et al. miR-149-3p Regulates the Switch between Adipogenic and Osteogenic Differentiation of BMSCs by Targeting FTO. *Mol Ther Nucleic Acids* 2019;17:590-600.
- Hua R, Zou J, Ma Y, et al. Psoralidin prevents caffeine-induced damage and abnormal differentiation of bone marrow mesenchymal stem cells via the classical estrogen receptor pathway. *Ann Transl Med* 2021;9:1245.
- Armada-Moreira A, Taipaleenmäki E, Baekgaard-Laursen

- M, et al. Platinum Nanoparticle-Based Microreactors as Support for Neuroblastoma Cells. *ACS Appl Mater Interfaces* 2018;10:7581-92.
25. Mou S, Zhou M, Li Y, et al. Extracellular Vesicles from Human Adipose-Derived Stem Cells for the Improvement of Angiogenesis and Fat-Grafting Application. *Plast Reconstr Surg* 2019;144:869-80.
  26. Wu Y, Gao Q, Zhu S, et al. Low-intensity pulsed ultrasound regulates proliferation and differentiation of neural stem cells through notch signaling pathway. *Biochem Biophys Res Commun* 2020;526:793-8.
  27. Murata K, Ito H, Yoshitomi H, et al. Inhibition of miR-92a enhances fracture healing via promoting angiogenesis in a model of stabilized fracture in young mice. *J Bone Miner Res* 2014;29:316-26.
  28. Hao J, Li B, Duan HQ, et al. Mechanisms underlying the promotion of functional recovery by deferoxamine after spinal cord injury in rats. *Neural Regen Res* 2017;12:959-68.
  29. Wang T, Li B, Wang Z, et al. Sorafenib promotes sensory conduction function recovery via miR-142-3p/AC9/cAMP axis post dorsal column injury. *Neuropharmacology* 2019;148:347-57.
  30. Iaquinta MR, Mazzoni E, Bononi I, et al. Adult Stem Cells for Bone Regeneration and Repair. *Front Cell Dev Biol* 2019;7:268.
  31. Hajiali H, Ouyang L, Llopis-Hernandez V, et al. Review of emerging nanotechnology in bone regeneration: progress, challenges, and perspectives. *Nanoscale* 2021;13:10266-80.
  32. Pittenger MF, Mackay AM, Beck SC, et al. Multilineage potential of adult human mesenchymal stem cells. *Science* 1999;284:143-7.
  33. da Silva Meirelles L, Caplan AI, Nardi NB. In search of the in vivo identity of mesenchymal stem cells. *Stem Cells* 2008;26:2287-99.
  34. Dawson JI, Kanczler J, Tare R, et al. Concise review: bridging the gap: bone regeneration using skeletal stem cell-based strategies - where are we now? *Stem Cells* 2014;32:35-44.
  35. James AW, Zara JN, Zhang X, et al. Perivascular stem cells: a prospectively purified mesenchymal stem cell population for bone tissue engineering. *Stem Cells Transl Med* 2012;1:510-9.
  36. Ciuffi S, Zonefrati R, Brandi ML. Adipose stem cells for bone tissue repair. *Clin Cases Miner Bone Metab* 2017;14:217-26.
  37. Danisovic L, Oravcova L, Krajciová L, et al. Effect of long-term culture on the biological and morphological characteristics of human adipose tissue-derived stem Cells. *J Physiol Pharmacol* 2017;68:149-58.
  38. Shaik S, Wu X, Gimble J, et al. Effects of Decade Long Freezing Storage on Adipose Derived Stem Cells Functionality. *Sci Rep* 2018;8:8162.
  39. Niemeyer P, Kornacker M, Mehlhorn A, et al. Comparison of immunological properties of bone marrow stromal cells and adipose tissue-derived stem cells before and after osteogenic differentiation in vitro. *Tissue Eng* 2007;13:111-21.
  40. Zhang J, Huang X, Wang H, et al. The challenges and promises of allogeneic mesenchymal stem cells for use as a cell-based therapy. *Stem Cell Res Ther* 2015;6:234.
  41. Meijer GJ, de Bruijn JD, Koole R, et al. Cell based bone tissue engineering in jaw defects. *Biomaterials* 2008;29:3053-61.
  42. Kulakov AA, Goldshtein DV, Grigoryan AS, et al. Clinical study of the efficiency of combined cell transplant on the basis of multipotent mesenchymal stromal adipose tissue cells in patients with pronounced deficit of the maxillary and mandibular bone tissue. *Bull Exp Biol Med* 2008;146:522-5.
  43. Levi B, James AW, Nelson ER, et al. Human adipose derived stromal cells heal critical size mouse calvarial defects. *PLoS One* 2010;5:e11177.
  44. Lee RH, Kim B, Choi I, et al. Characterization and expression analysis of mesenchymal stem cells from human bone marrow and adipose tissue. *Cell Physiol Biochem* 2004;14:311-24.
  45. Pajarinen J, Lin T, Gibon E, et al. Mesenchymal stem cell-macrophage crosstalk and bone healing. *Biomaterials* 2019;196:80-9.
  46. Al-Ghadban S, Bunnell BA. Adipose Tissue-Derived Stem Cells: Immunomodulatory Effects and Therapeutic Potential. *Physiology (Bethesda)* 2020;35:125-33.
  47. Oryan A, Kamali A, Moshiri A, et al. Role of Mesenchymal Stem Cells in Bone Regenerative Medicine: What Is the Evidence? *Cells Tissues Organs* 2017;204:59-83.
  48. Li Y, Liu C. Nanomaterial-based bone regeneration. *Nanoscale* 2017;9:4862-74.
  49. Kim WK, Kim JC, Park HJ, et al. Platinum nanoparticles reduce ovariectomy-induced bone loss by decreasing osteoclastogenesis. *Exp Mol Med* 2012;44:432-9.
  50. Gurunathan S, Jeyaraj M, Kang MH, et al. The Effects of Apigenin-Biosynthesized Ultra-Small Platinum

Nanoparticles on the Human Monocytic THP-1 Cell Line. *Cells* 2019;8:444.

51. Nomura M, Yoshimura Y, Kikuri T, et al. Platinum nanoparticles suppress osteoclastogenesis through

scavenging of reactive oxygen species produced in RAW264.7 cells. *J Pharmacol Sci* 2011;117:243-52.

(English Language Editor: A. Kassem)

**Cite this article as:** Chen CJ, Feng Y, Jin L, Wang X, Xu LX, Lin JM, Feng LW, Liu LN, Hou Z. Adipose-derived mesenchymal stem cells combined with platinum nanoparticles accelerate fracture healing in a rat tibial fracture model. *Ann Transl Med* 2022;10(8):450. doi: 10.21037/atm-22-1196